Histochem Cell Biol (2012) 137:217–233
DOI 10.1007/s00418-011-0889-9

ORIGINAL PAPER

Immunodetection of cyclooxygenase-2 (COX-2) is restricted to tissue macrophages in normal rat liver and to recruited mononuclear phagocytes in liver injury and cholangiocarcinoma

Marta Wójcik · Pierluigi Ramadori · Martina Blaschke · Sadaf Sultan · Sajjad Khan · Ihtzaz A. Malik · Naila Naz · Gesa Martius · Giuliano Ramadori · Frank C. Schultze

Accepted: 13 November 2011 / Published online: 1 December 2011

Abstract It has been suggested that cyclooxygenase-2 (COX-2)-mediated prostaglandin synthesis is associated with liver inflammation and carcinogenesis. The aim of this study is to identify the cellular source of COX-2 expression in different stages, from acute liver injury through liver fibrosis to cholangiocarcinoma (CC). We induced in rats acute and "chronic" liver injury (thioacetamide (TAA) or carbon tetrachloride (CCl_4)) and CC development (TAA) and assessed COX-2 gene expression in normal and damaged liver tissue by RT-PCR of total RNA. The cellular localization of COX-2 protein in liver tissue was analyzed by immunohistochemistry as well as in isolated rat liver cells by Western blotting. The findings were compared with those obtained in human cirrhotic liver tissue. The specificity of the antibodies was tested by 2-DE Western blot and mass spectrometric identification of the positive protein spots. RT-PCR analysis of total RNA revealed an increase of hepatic COX-2 gene expression in acutely as well as "chronically" damaged liver. COX-2-protein was detected in those $ED1^+/ED2^+$ cells located in the non-damaged tissue (resident tissue macrophages). In addition COX-2 positivity in inflammatory mononuclear phagocytes ($ED1^+/ED2^-$), which were also present within the tumoral tissue was detected. COX-2 protein was clearly detectable in isolated Kupffer cells as well as (at lower level) in isolated "inflammatory" macrophages. Similar results were obtained in human cirrhotic liver. COX-2 protein is constitutively detectable in liver tissue macrophages. Inflammatory mononuclear phagocytes contribute to the increase of COX-2 gene expression in acute and chronic liver damage induced by different toxins and in the CC microenvironment.

Keywords COX-2 · Macrophages · Kupffer cells · Liver injury · Cholangiocarcinoma

Abbreviations

CC	Cholangiocarcinoma
COX-2	Cyclooxygenase-2
TAA	Thioacetamide
CK-19	Cytokeratin-19

Introduction

COX-1 and COX-2 are two isoforms of the enzyme cyclooxygenase (COX), also known as prostaglandin H synthase (PGHS) or prostaglandin endoperoxide synthase (PTGS). Both COX isoforms are associated with inner membranous compartments (Bayly et al. 1999; Picot et al.

Two brief statements Expression of cyclooxygenase-2 (COX-2) is restricted to tissue macrophages and to recruited mononuclear phagocytes in rat liver injury and cholangiocarcinoma. Our results indicate that the targets of COX-2 inhibitors are not the tumor cells themselves, but the tissue macrophages of the tumor microenvironment.

Electronic supplementary material The online version of this article (doi:10.1007/s00418-011-0889-9) contains supplementary material, which is available to authorized users.

M. Wójcik · P. Ramadori · M. Blaschke · S. Sultan · S. Khan · I. A. Malik · N. Naz · G. Martius · G. Ramadori (✉) · F. C. Schultze
Department of Gastroenterology and Endocrinology, University Medical Center Goettingen, Robert-Koch-Str. 40, 37075 Goettingen, Germany
e-mail: gramado@med.uni-goettingen.de

M. Wójcik
Chair of Preclinical of Veterinary Sciences, Department of Pathophysiology, Faculty of Veterinary Medicine, University of Life Sciences in Lublin, Lublin, Poland

1994) and represent key enzymes in the conversion of arachidonic acid to prostaglandin (PG). COX-1 is constitutively expressed in most cell types and is involved in the homeostasis of various physiological functions, while COX-2 is considered to be a mitogen-inducible form, associated with biologic events such as injury, inflammation, and proliferation (O'Banion et al. 1991, 1992; Kirschenbaum et al. 2000). COX-2 gene expression was demonstrated in vitro in different cell types, e.g. in monocytes, human umbilical vein endothelial cells, vascular smooth muscle cells, and fibroblasts (Hla and Neilson 1992), but only a few data are available for tissue macrophages (Ahmad et al. 2002).

COX-2-derived PGE_2 can stimulate angiogenesis by induction of the vascular endothelial growth factor (Simmons et al. 2004; Tsujii et al. 1998). Furthermore, it has been shown that tumor angiogenesis and growth of explanted tumors are reduced in COX-2 null mice (Williams et al. 2000). PGE_2 also has an effect on the immune system by regulating cytokine production in leukocytes (Betz and Fox 1991; Kunkel et al. 1986a; Kunkel et al. 1988; Kunkel et al. 1986b). Bennett et al. (1977) showed that large amounts of PGs are produced by certain tumor cells and it has been suggested that PGE_2 is associated with cancer through depression of the immune system (Simmons et al. 2004). It is therefore believed that COX-2 plays an important role in carcinogenesis and COX-2 has been studied extensively as a key rate-limiting enzyme for prostanoid biosynthesis.

COX-2 has been implicated in the carcinogenesis of various human cancers, including colorectal cancer and also CC (Endo et al. 2002; Gasparini et al. 2003; Hu 2003; Han et al. 2004; Han and Wu 2005; Wu 2005; Eisinger et al. 2007; Zhang et al. 2005). In many cases, however, the presence of mononuclear phagocytes in the tumor samples has not been considered.

Several conflicting reports exist in the literature about COX-2 expression in liver. For example, some publications described COX-2 immunodetection in normal or damaged hepatocytes, and it has been suggested that COX-2 expression could be related to the inflammatory phenomena present in the early phases of different chronic liver diseases and is probably also related to the induction of hepatocarcinogenesis (Chariyalertsak et al. 2001; Giannitrapani et al. 2009) while others have established that adult hepatocytes fail to express the COX-2 gene (Casado et al. 2007; Mohammed et al. 2004). Furthermore, COX-2 positivity has been described in CC cells by immunohistology using immunoperoxidase staining (Endo et al. 2002).

COX-2 has attracted particular interest because of the cancer preventive and therapeutic potential of its inhibition and because of its possible role in the early phases of CC development. Furthermore, in several reports it has been assumed that malignant cells became able to express the COX-2 gene and that these cells may be the target of COX-2 inhibitors (Zhang et al. 2004; Thakur and Sanyal 2010). In fact, it has been shown that COX-2 inhibitors reduced the in vitro growth of 5 human COX-2-expressing CC cell lines (Zhang et al. 2004).

We recently established an animal model of CC in the rat by administering TAA in drinking water which have morphological similarities with CC observed in human pathology (Mansuroglu et al. 2009a,b). We investigated the expression of COX-2 at various stages of acute and chronic liver injury up to CC development using this model. Moreover, we worked at identifying the cell type(s) expressing COX-2 in the same rat liver. For comparison one other rat model of hepatocellular damage and inflammation was used. In addition, human liver tissue samples were also studied. We found that COX-2 protein is constitutively expressed in liver tissue macrophages and that the increased expression during inflammation is however not only due to an upregulation of the gene in those cells but newly recruited inflammatory mononuclear phagocytes also contribute to increased COX-2 gene expression. Neither hepatocytes nor CC cells seem to be able to express COX-2 in this experimental setting.

Materials and methods

Chemicals and antibodies

The majority of the chemicals and solutions used were purchased from Sigma (Steinheim, Germany): DL-dithiothreitol (DTT), lipopolysaccharide (LPS), phenylmethylsulfonyl fluoride (PMSF), phorbol 12-myristate 13-acetate (PMA), phosphatase inhibitor cocktail 1 and 2, TAA, thiourea, urea; from Merck KGaA (Darmstadt, Germany): glycerine, HCl; from PAA Laboratories GmbH (Cölbe, Germany) we purchased: RPMI 1640 medium, fetal calf serum (FCS), penicillin/streptomycin, and phosphate-buffered saline (Dulbecco's PBS); were obtained from Biochrom AG (Berlin, Germany): medium M199, L-glutamine and from Bio-Rad (Munich, Germany): a Bio-Rad protein assay kit and ampholytes (Bio-Lyte® 3/10). Bromphenol blue and Tris came from Carl Roth GmbH (Karlsruhe, Germany) and 3-[(3-cholamidopropyl) dimethylammonio]-1-propanesulfonate (CHAPS) from AppliChem GmbH (Darmstadt, Germany). Bovine serum albumin (BSA) and sodium dodecyl sulfate were purchased from Serva (Heidelberg, Germany). Primer pairs of COX-2, ED1, ubiquitin C (UBC), protector RNAse inhibitor, and 1x RT buffer were supplied by Invitrogen (Darmstadt, Germany). Fast Sybr Green master mix was supplied by AB (Applied Biosystem, USA). 4',6-diamidino-2-phenylindole (DAPI) was delivered by Molecular Probes (Leiden, The

Table 1 The antibodies used in this study

Clone	Specificity	Applications	Dilution	Source
33/Cox-2	Anti-COX-2 mouse monoclonal	WB: 1D, 2D	1:100, 1:100	BD Transduction Laboratories (Heidelberg, Germany)
		IHC	1:50	
–	Anti-COX-2 (H-62; sc-7951) rabbit polyclonal	WB: 2D	1:100	Santa Cruz Biotechnology (Heidelberg, Germany)
–	Anti-COX-2 (N-20; sc-1746) goat polyclonal	WB: 2D	1:100	
–	Anti-COX-2 (ab15191) rabbit polyclonal	WB: 1D, 2D	1:100, 1:100	Abcam plc (Cambridge, UK)
		IHC	1:100	
b170	Anti-CK-19 mouse monoclonal	IHC	1:50	Leica Biosys. Newcastle Ltd. (Newcastle, UK)
OCH1E5	Anti-Hep Par-1 mouse monoclonal	IHC	1:50	DAKO (Hamburg, Germany)
PG-M1	Anti-human CD68 mouse monoclonal	IHC	1:100	
ED1	Anti-ED1 mouse monoclonal	WB: 1D	1:200	AbD Serotec (Oxford, UK)
		IHC	1:50	
ED2	Anti-ED2 mouse monoclonal	IHC	1:50	
Secondary antibodies				
Polyclonal rabbit anti-mouse immunglobulins/HRP		WB: 1D, 2D	1:1,000	DAKO (Hamburg, Germany)
Polyclonal rabbit anti-goat immunglobulins/HRP		WB: 1D, 2D	1:1,000	
Polyclonal swine anti-rabbit immunglobulins/HRP		WB: 1D, 2D	1:1,000	
AlexaFluor-555-conjugated goat anti-rabbit IgG		IHC	1:1,000	Molecular Probes (Leiden, The Netherland)
AlexaFluor-488-conjugated goat anti-mouse IgG		IHC	1:500	
APAAP consists of soluble complexes of calf intestinal alkaline phosphatase and mouse monoclonal anti-alkaline phosphatase				
AP7/6/7	Anti-alkaline phosphatase mouse monoclonal	IHC	1:20	DAKO (Hamburg, Germany)
–	Rabbit anti-mouse immunglobulins (Z 0259)	IHC	1:20	

Netherland) and moloney murine leukaemia virus reverse transcriptase (M-MLV RT) by Promega (Mannheim, Germany). The antibodies used in this study are shown in Table 1.

Animals

Male Sprague–Dawley rats weighing 330–370 g were used for TAA and CCl_4 experiments; they were provided by Charles River (Sulzfeld, Germany) and Harlan Winkelmann (Borchen, Germany). The animals were kept under standard conditions with 12-h light/dark cycles; food and water were available ad libitum and they received care according university policies and the relevant guidelines for care and use of laboratory animals of the German National Institute of Health. All animal experiments performed were approved by the ethics review board and were constantly supervised by the local ethics commission. Animals of all experimental groups were killed under pentobarbital anesthesia. Livers were rinsed and snap-frozen in liquid nitrogen. Samples were stored at −80°C until further use. All experiments were repeated in three series. Four animals were killed at each time point.

Induction of acute liver injury, liver fibrosis, and CC development by TAA

Acute liver damage was induced by a single intraperitoneal (i.p.) injection of TAA dissolved in sterile sodium saline. Control rats received only a single i.p. injection of sterile sodium saline. Four animals in each group were killed 1, 3, 6, 12, 24, 48, 72 and 96 h after a single-dose TAA administration.

Induction of liver fibrosis and CC by TAA administration was conducted according to Yeh et al. (2008) as described elsewhere (Mansuroglu et al. 2009a, b). Animals were divided into two groups, i.e. a control group and an experimental group. The experimental group received TAA in their drinking water every day up to the time they were euthanized. Four animals in each group were killed at various time points. By week 16, 80% of the TAA-treated rats had developed CC and the experiment was stopped at week 18, when 100% of the TAA-treated rats had developed CC.

Induction of acute and chronic liver injury by CCl_4

Acute liver damage was induced by orally administered CCl_4 as described previously (Knittel et al. 1999; Neubauer

et al. 1995). A single dose of 150 µl CCl_4/corn oil solution (50%, v/v) per 100 g body weight was given to each rat. Control rats received only corn oil. Rats were killed 3, 6, 9, 12, 24, 48, 72, and 96 h after the CCl_4 administration.

Chronic liver injury was induced according to the protocol by Proctor and Chatamra (1982). The experimental group received CCl_4 orally once a week. After a period of 8 and 13 weeks, the animals were killed and livers were obtained.

Isolation of hepatocytes, tissue macrophages (Kupffer cells), and myofibroblasts from rat livers

Hepatocytes from male Sprague–Dawley rats were isolated by in situ perfusion and cultured as reported previously (Neubauer et al. 1995; Knittel et al. 1992). Kupffer cells and myofibroblasts of normal liver were isolated as described by Knook and Sleyster (1976) with some modifications (Armbrust et al. 1993; Neubauer et al. 2008).

Isolated cells were cultured for 24 h and protein extracts were prepared from Kupffer cells, hepatocytes, and myofibroblasts. For mRNA isolation, Kupffer cells (in duplicate) were stimulated with 10 µg/ml LPS, and mRNA was obtained 2, 4, and 6 h from LPS-treated as well as from control cultures.

Isolation of mononuclear phagocytes from damaged rat livers

Mononuclear phagocytes from TAA- and CCl_4-damaged rat livers were isolated by in situ perfusion. Centrifugal elutriation was performed to separate small KC from large KC. The first fraction was collected at flow rates ranging from 19 up to 28 ml/min (Beckmann centrifuge J2-21, J-6B rotor, 2,500 rpm) and the second fraction at flow rates ranging from 28 up to 55 ml/min. Each fraction was sedimented, resuspended in culture medium (M199, 15% FCS, 100 U penicillin/ml, 100 µg streptomycin/ml), and counted in a Neubauer chamber after Trypan Blue-staining. Cells were then plated onto 24-well plates (5×10^5 cells/well). Two hours after plating, the cultures were washed intensively to eliminate non-adherent cells. Cultures were kept in a 5% CO_2 atmosphere and saturated humidity at 37°C. Total protein extracts and mRNA were obtained.

Human liver tissue

Four specimens of cirrhotic human livers were obtained from patients undergoing transplantation after developing HCC or CC and four specimens of cirrhotic liver without tumor. Specimens were frozen in liquid nitrogen immediately after surgical removal. Human liver samples were used for immunohistochemical analysis.

Culture and activation of macrophage cell line

The monocytic/macrophage cell line RAW 264.7 (Lüder et al. 2003; Raschke et al. 1978) was a gift from the Department of Bacteriology, Georg-August University Goettingen (UMG, Goettingen, Germany). RAW 264.7 cells were incubated with RPMI 1640 medium containing 10% FCS, 100 U/ml penicillin, 100 mg/ml streptomycin, 2 mmol/l L-glutamine, and 2.5 g/l D-glucose at 37°C, 20% O_2, and 5% CO_2. Cells were used to determine the specifity of COX-2 antibody binding and the effect of stimulation on COX-2 expression. Cells were activated with 10 µg/ml LPS and 10 ng/ml PMA. PMA was dissolved in DMSO (0.5 mg/ml) and aliquots were stored at −20°C; LPS was dissolved in PBS. Control cells were incubated with the DMSO vehicle only. For protein or mRNA isolation, cells were seeded at 0.2×10^7 cells in 75 cm^2 tissue culture flasks (Sarstedt AG & Co., Nümbrecht, Germany).

RNA isolation and real-time PCR

RNA was isolated from all control and TAA-treated rat livers. RNA quality was tested by agarose gel electrophoresis and visualized with UV light. RNA concentration was quantified by measuring the absorbance at 260/280 nm. The cDNA was generated by reverse transcription of 3.0 µg of total RNA with 100 nmol/l of dNTPs, 50 pmol/l of primer oligo(dT)15, 200 units of M-MLV RT, 16 units of protector RNAse inhibitor, 1× RT buffer, and 2.5 ml of 0.1 mol/l DTT for 1 h at 40°C as described previously (Kondo et al. 1999). Gene expression of COX-2 (forward primer 5′-TAC CGGACTGGATTCTAG-3′, reverse primer 5′-AAGTTG GTGGGCTGTCAATC-3′), and ED1 (forward primer 5′-A TTGAACCCGAACAAAACCA-3′, reverse primer 5′-GC TTGTGGGAAGGACACATT-3′) were analyzed using a Fast Sybr Green master mix. UBC (forward primer 5′-CAC CAAGAAGGTCAAACAGGAA-3′, reverse primer 5′-AA GACACCTCCCCATCAAACC-3′) was used as housekeeping gene in the TAA model. The amplification was performed through two-step cycling (95–60°C) for 40 cycles in a StepOne Plus RT-PCR detection system, following the instructions of the supplier (AB, Applied Biosystem, USA). All samples were assayed in duplicate. The results were normalized to the controls, and fold change of the gene expression was calculated using threshold cycle (Ct) values.

Total protein extraction from rat liver, isolated rat liver cells, and monocytic/macrophage cell line RAW 264.7

Total protein extracts were prepared from all controls, TAA/CCl_4-treated rat livers, and dissected CC tissues, as well as from isolated hepatocytes, myofibroblasts, Kupffer

cells, and RAW 264.7 cells. Tissues were washed in ice-cold PBS to remove blood and homogenized at room temperature in cell lysis buffer containing 7 mol/l urea, 2 mol/l thiourea, 4% (w/v) CHAPS, 2% ampholytes, 1% (w/v) DL-dithiothreitol and 10 mmol/l phenylmethylsulphonyl fluoride, as well as 1% (v/v) phosphatase inhibitor cocktail 1, and 1% (v/v) phosphatase inhibitor cocktail 2 with a homogenizer (Ultra-Turrax, Jahnke and Kunkel GmbH & CO.KG, Staufen, Germany). The protein concentration was calculated according to Bradford (1976) using the Bio-Rad protein assay kit. The protein samples were stored at −80°C until further analysis.

1-DE/2-DE Western blot analysis of total protein lysates from rat liver tissue, isolated rat liver cells, and RAW 264.7cells

For 1-DE Western blot analysis, 50 µg total protein was loaded on a 4–12% NuPAGE Bis–Tris gel (Invitrogen, Darmstadt, Germany) and separated for 2 h by electrophoresis at 80 V. For 2-DE Western blot analysis, 140 µg total protein lysate from rat liver tissues or from macrophage cell line RAW 264.7 and a trace of bromphenol blue were loaded on immobilized pH gradient (IPG) strips with a nonlinear pH range of 3–10. After rehydration, isoelectric focusing was performed in a Protein IEF Cell (Bio-Rad) at 20°C set to 32,000 Vh. The IPG strip was equilibrated with equilibration buffer (6 mol/l urea, 30% glycerine, 2% sodium dodecyl sulphate, 0.05 mol/l Tris/5 N HCl to pH 8.8 and a trace of bromophenol blue) containing 15 mmol/l DTT, followed with equilibration buffer containing 40 g/l iodoacetamide. Afterwards, the strip was loaded onto a vertical 12% polyacrylamide SDS-PAGE for separation by molecular weight for 19 h at 4°C and 90 V. After Western blot, Ponceau staining was performed as a control for successful protein transfer. Nitrocellulose membranes were blocked in blocking buffer containing 5% BSA and were incubated overnight at 4°C with different anti-COX-2 antibodies (33/Cox-2, ab15191, sc-1746, sc-7951). The secondary antibodies were conjugated with horseradish peroxidase. The membranes were developed with an ECL chemiluminescence kit (GE Healthcare, Munich, Germany). Antibodies and dilutions used are listed in Table 1.

Silver-staining of proteins

2-DE gels were fixed and washed and silver-staining was performed according to the modified silver-staining method of Blum et al. (1987). Gels were scanned (CanoScan 8400F, Canon) and finally dried for further storage (Gel Dryer, Model 583; Bio-Rad).

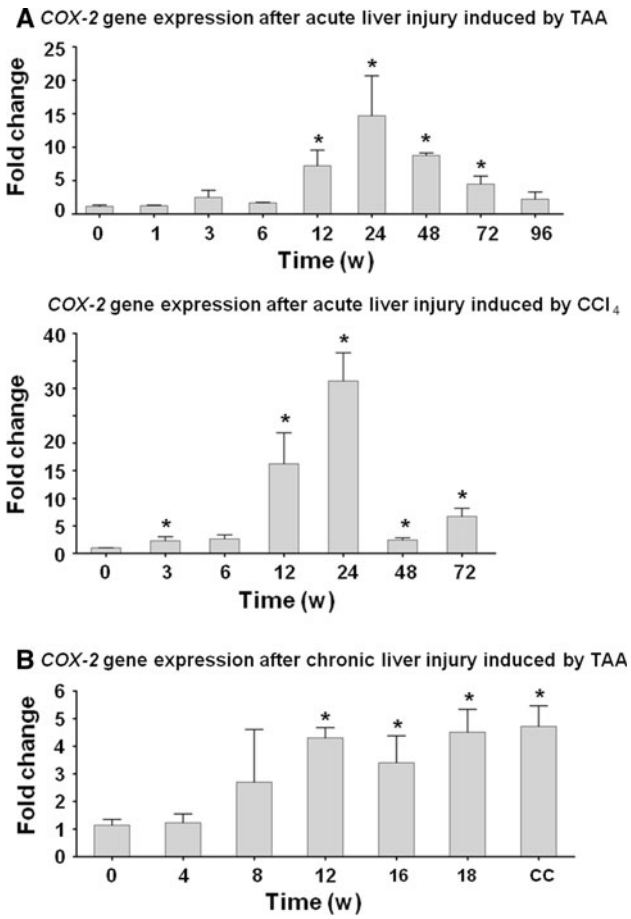

Fig. 1 Changes of COX-2 gene expression in rat liver tissue are shown at various time points during (**a**) acute liver injury after TAA (*top*) or CCl_4 (*bottom*) administration and (**b**) chronic liver injury as well as in dissected CC tissue after TAA administration. *The graphics* represent the COX-2-specific mRNA amount normalized using UBC as housekeeping gene. *Error bars* represent standard deviation (control 0 h $n = 4$, treatment $n = 4$, CC $n = 4$). *h* hours, *w* weeks, *CC* dissected cholangiocarcinoma tissue, $^*P < 0.05$ against control group according to the Mann–Whitney *U* test

Protein identification

In-gel digestion was carried out according to a modified protocol of Shevchenko et al. (1996). Spots of interest were the positive spots from the ECL staining after 2-DE blots. These were excised and after de-staining with potassium ferricyanide and sodium thiosulphate; proteins/peptides were digested with trypsin. Gel slices were washed and equilibrated with ammonium bicarbonate followed by incubation with acetonitrile (ACN). Peptides were extracted using trifluoroacetic acid and ACN. Solutions with digested protein/peptide were dried in a speed vacuum system (UniEquip GmbH, Munich, Germany) and stored at −20°C

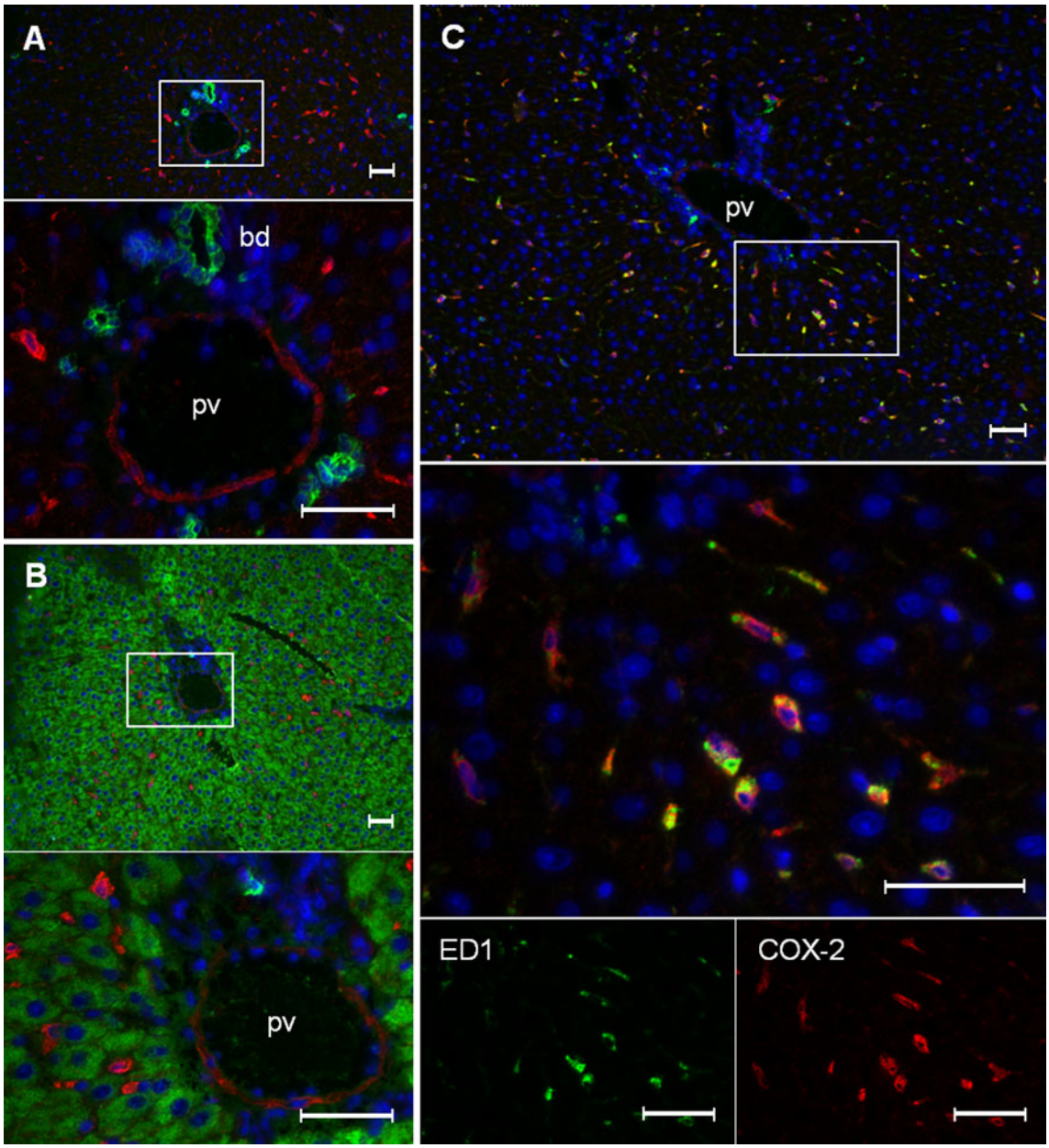

Fig. 2 Immunolocalization of COX-2 protein by double immunofluorescence staining (CK-19, Hep Par-1, and ED1) in normal rat liver. Immunofluorescence staining of **a**: COX-2 (*red*) and CK-19 (*green*); **b**: COX-2 (*red*) and Hep Par-1 (*green*); **c**: COX-2 (*red*) and ED1 (*green*). Co-localization of COX-2 and ED1 is detectable. Polyclonal COX-2 antibody (ab15191) was used. The blue staining with DAPI represents the nuclei (×100/×400 original magnification). *pv* portal vein, *bd* bile duct. *Bar* 50 µm

until further analysis. Dried samples were diluted in 0.1% formic acid and 1 µl was loaded for chromatographic separation on a CapLC-System (Waters, Milford, MA, USA). Peptide sequence analysis was carried out on a Q-TOF Ultima Global mass spectrometer (Micromass, Manchester, UK) equipped with a nanoflow ESI Z-spray source in positive ion mode, as described previously (Schultze et al. 2010). Data were processed using Protein Lynx Global Server (2.0, Micromass) and searched against MSDB and SwissProt data bases through the Mascot search engine with oxidation (M) and carbamidomethyl (C) modification, when appropriate.

Histochemical analysis and immunohistochemical investigations

Tissue sections were first analyzed by hematoxylin and eosin staining (HE). Liver tissue sections (5 µm thick) of three representative rats as well as three control rats were analyzed at the following time points: 0, 24, 48, 96 h, 8,

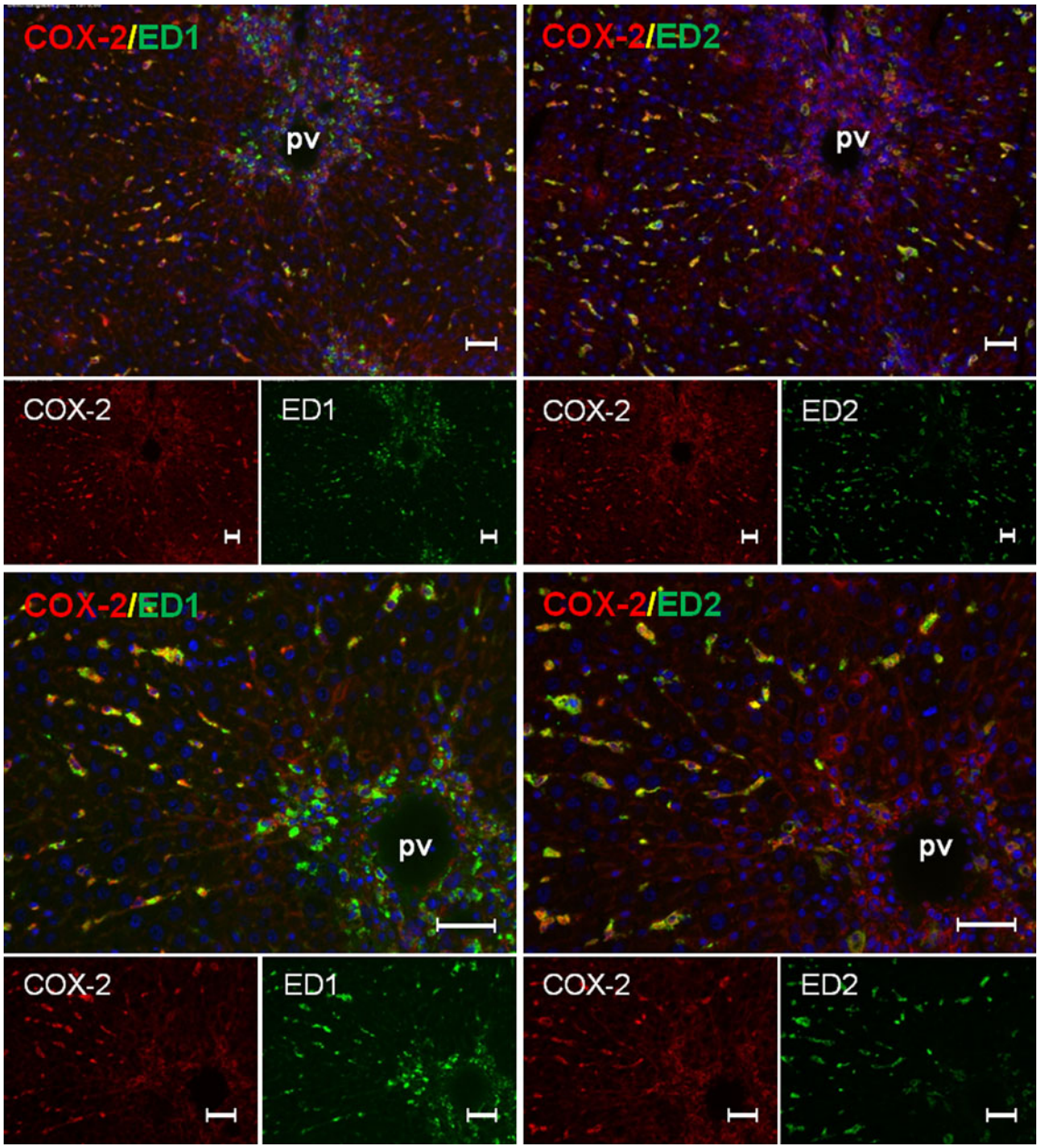

Fig. 3 Immunolocalization of COX-2, ED1 and ED2 in TAA-induced acute rat liver injury (48 h). An immunofluorescence staining of COX-2- (*red*), ED1- (*green*, *left side*), and ED2$^-$ (*green*, *right side*) positive cells is shown. Polyclonal COX-2 antibody (ab15191) was used. Staining with DAPI represents the nuclei (×100/×200 original magnification). *pv* portal vein. *Bar* 50 µm

16, and 18 weeks. Furthermore, specimens of four cirrhotic human livers after developing HCC or CC and four specimens of cirrhotic liver without tumor were analyzed. After blocking of non-specific binding with 1% BSA and 10% goat serum (DAKO, Hamburg, Germany) containing PBS for 1 h at room temperature, two primary antibodies were simultaneously incubated on the sections overnight at 4°C. We used primary antibodies: rabbit polyclonal anti-COX-2; mouse monoclonal anti-COX-2 (33/Cox-2), mouse monoclonal anti-CK-19; mouse monoclonal anti-Hep Par-1; mouse monoclonal anti-ED1, mouse monoclonal anti-CD68, and mouse monoclonal anti-ED2. Rabbit polyclonal antibodies were detected with AlexaFluor-555-conjugated goat anti-rabbit secondary antibody and mouse monoclonal antibodies were visualized with AlexaFluor-488-conjugated goat anti-mouse secondary antibody. Antibody dilutions used are listed in Table 1.

In the double staining immunohistochemistry, ED1$^+$/COX-2$^+$ positive cells were counted in five randomly selected areas (0.51 mm^2/area) in the centrilobular area of the hepatic lobule at a magnification of 100×.

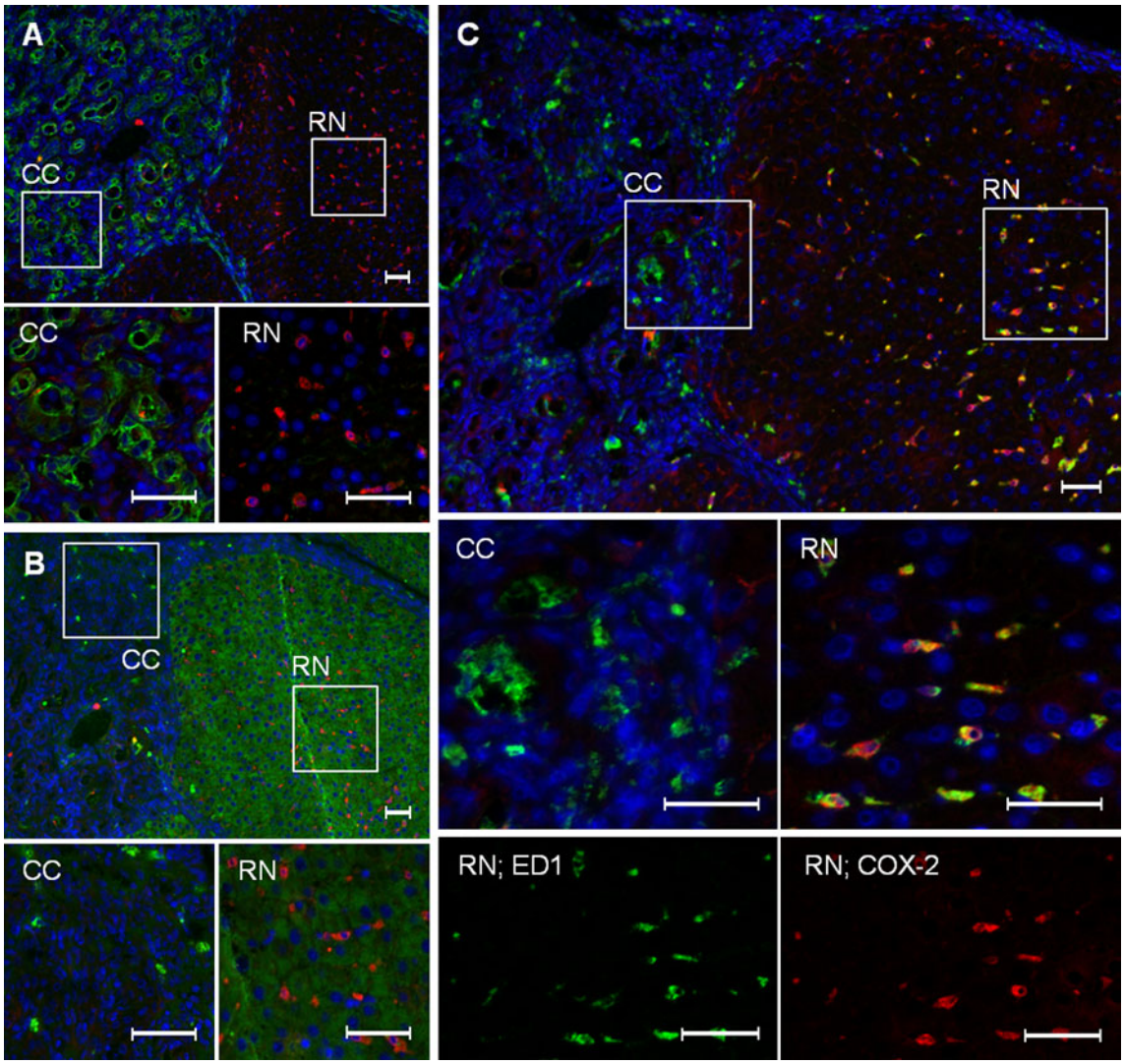

Fig. 4 Immunolocalization of COX-2, CK-19, Hep Par-1, and ED1 in TAA-induced chronic rat liver injury (16 weeks). Immunofluorescence staining of **a**: COX-2 (*red*) and CK-19 (*green*); **b**: COX-2 (*red*) and Hep Par-1 (*green*); **c**: COX-2 (*red*) and ED1 (*green*). Co-expression of COX-2 and ED1 is detectable only within regenerating nodules. Polyclonal COX-2 antibody (ab15191) was used. The blue staining with DAPI represents the nuclei (×100/×400 original magnification). *RN* regenerating nodules, *CC* cholangiocarcinoma. *Bar* 50 μm

Negative control immunostainings were performed by omission of the primary antibodies, use of non-immune serum, and by isotype matching control immunoglobulin. Sections were counter-stained with DAPI and observed with an epifluorescence microscope (Axiovert 200 M, Zeiss, Jena, Germany).

Alkaline phosphatase anti-alkaline phosphatase (APAAP) technique

We used the mouse monoclonal anti-COX-2 antibody (33/Cox-2) in this experiment. To make the antigen (COX-2)/antibody reaction visible, the APAAP technique was performed (Cordell et al. 1984). The APAAP complex is stained with neufuchsin, which stains the COX-2-positive cells red. The remaining tissue is made visible by counter-staining with hematoxylin.

Statistical analysis

The data were analyzed with GraphPad Prism 4.0 software (San Diego, USA) and SPSS (V14.0 for Windows; Chicago, IL, USA). The results are shown as means ± standard deviation. Significant difference was assessed at $P < 0.05$ against the control group and calculated according to the Mann–Whitney *U* test.

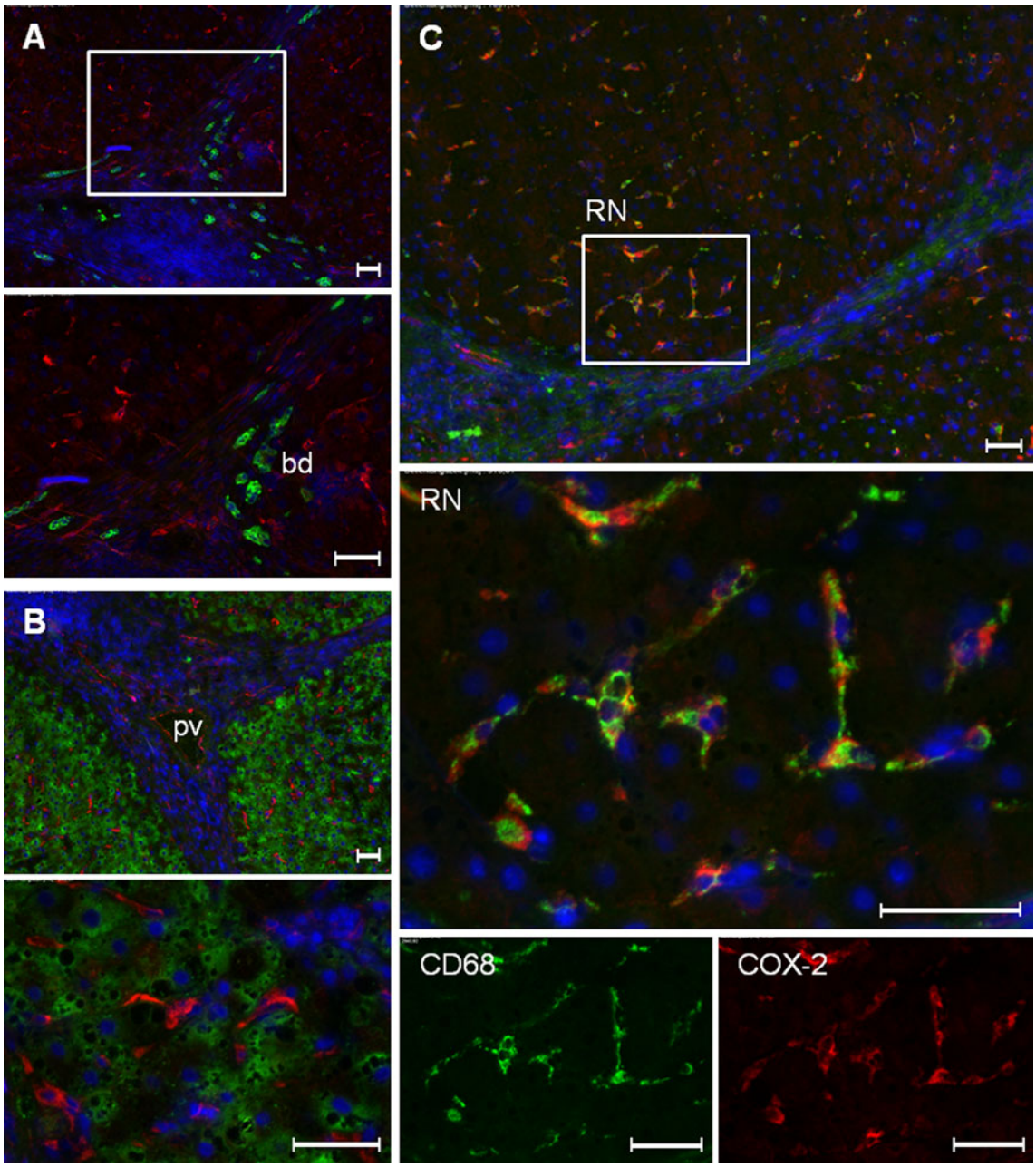

Fig. 5 Immunolocalization of COX-2, CK-19, Hep Par-1, and CD68 in cirrhotic human liver. Immunofluorescence staining of **a**: COX-2 (*red*) and CK-19 (*green*); **b**: COX-2 (*red*) and Hep Par-1 (*green*); **c**: COX-2 (*red*) and CD68 (*green*). Co-expression of COX-2 and CD68 is detectable only within regenerating nodules. Polyclonal COX-2 antibody (ab15191) was used. The blue staining with DAPI represents the nuclei (×100/×400 original magnification). *pv* portal vein, *bd* bile duct, *RN* regenerating nodule. *Bar* 50 μm

Results

COX-2 gene expression in normal and damaged rat liver

COX-2 specific mRNA

COX-2 mRNA was detectable in normal liver tissue and an upregulation up to 15-fold was detected during acute (Fig. 1a) and chronic liver injury (Fig. 1b). Significant upregulation of *COX-2* gene expression ($P < 0.05$) during acute liver injury was observed 12 h (7.2 ± 2.3-fold), 24 h (14.69 ± 5.99-fold), 48 h (8.76 ± 0.36-fold), and 72 h (4.48 ± 1.2-fold) after TAA administration. Chronic liver injury revealed significant upregulation ($P < 0.05$) after 12 weeks (4.31 ± 0.65-fold), 16 weeks (3.56 ± 0.65-fold), and 18 weeks of TAA administration (4.34 ± 1.94-fold), as well as in dissected CC tissue (4.94 ± 1.78-fold).

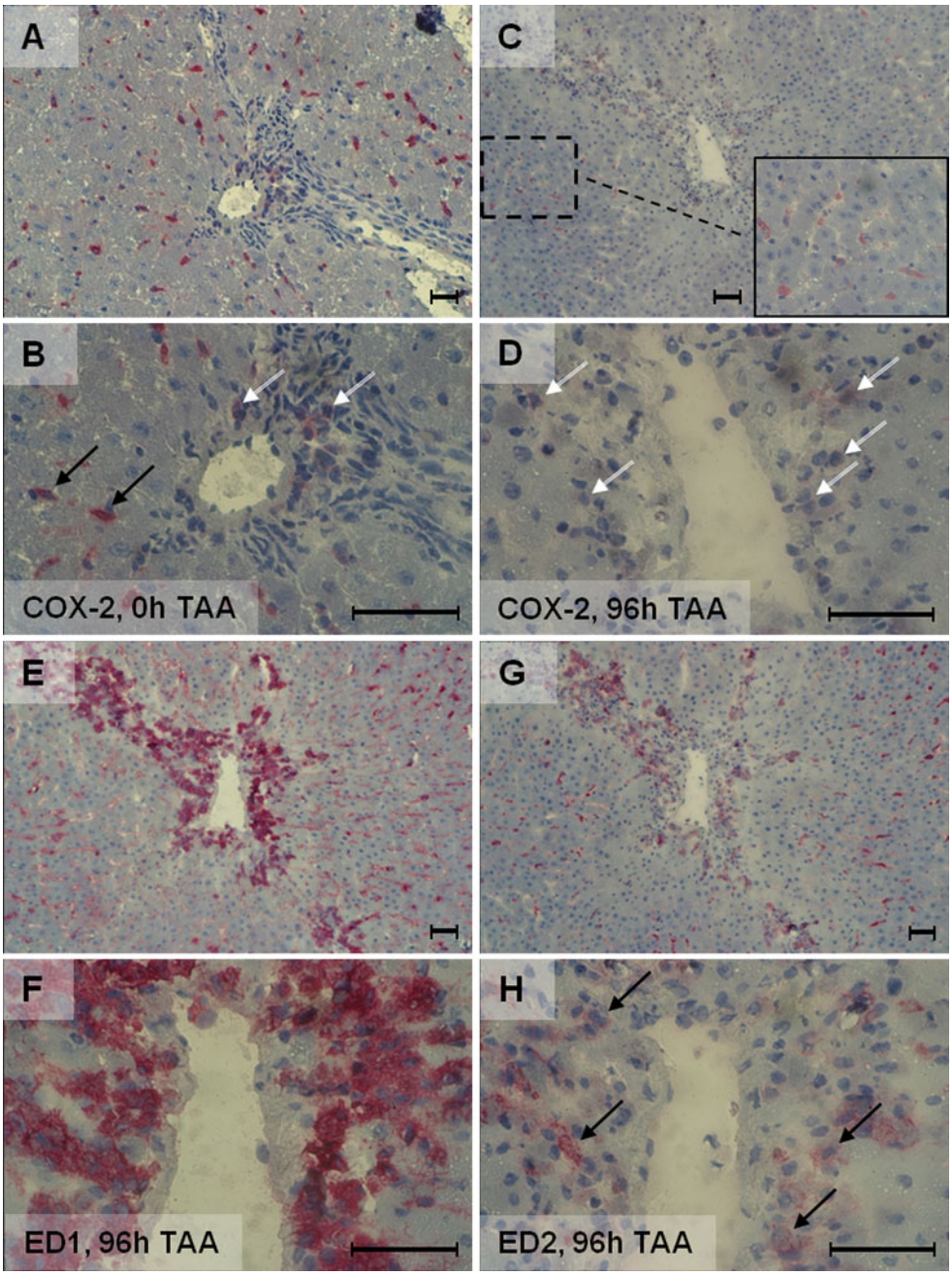

Fig. 6 Immunolocalization of COX-2 after TAA-induced acute rat liver injury (96 h). The following antibodies were used for immunohistological staining: monoclonal COX-2 antibody (33/Cox-2), monoclonal ED1 antibody (ED1) and monoclonal ED2 antibody (ED2). To visualize the antigen/antibody reaction, the classic alkaline phosphatase antialkaline phosphatase (APAAP) technique was used. The remaining tissue is made visible by counterstaining with hematoxylin. **a** COX-2 in the undamaged liver of a control animal (100-fold magnification). **b** Detail of **a** (400-fold magnification): a distinct COX-2 positivity is seen in cells (tissue macrophages) within the liver parenchyma (*black arrows*). Scattered cells with a weak positivity can be seen (*white arrows*) in the area of the portal field. **c** COX-2 after TAA-induced acute rat liver injury (96 h). **d** Detail of **c** (400-fold magnification): A weak COX-2 positivity is detectable in cells in the area of injury (*white arrows*). **e** Serial section. In the area of damage a variety of cells (recruited inflammatory macrophages) with a significant ED1 positivity can be detected. **f** Detail of e (400-fold magnification). **g** Serial section. ED2-positive cells are detectable in the area of injury. The intensity in the area of injury is lower than in the area of the undamaged parenchyma. **h** Detail of **g** (400-fold magnification). A weak ED2 positivity is detectable in cells in the area of injury (*black arrows*). *Bar* 50 µm

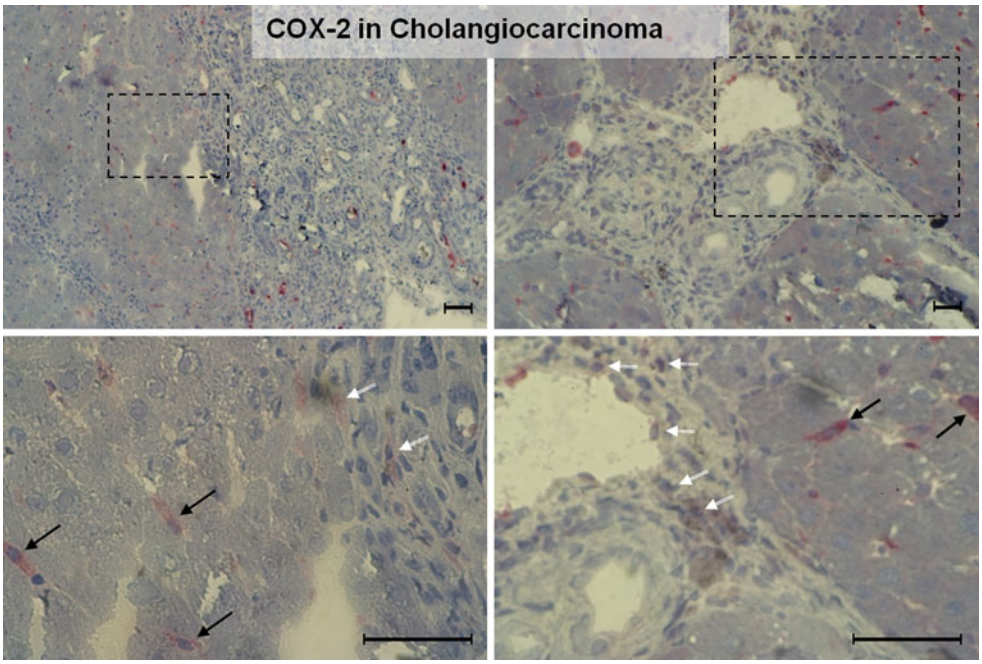

Fig. 7 Immunolocalization of COX-2 in TAA-induced cholangiocarcinoma. For immunostaining the monoclonal COX-2 antibody (33/Cox-2) was used. To visualize the antigen/antibody reaction, the classic alkaline phosphatase antialkaline phosphatase (APAAP) technique was used. The remaining tissue is made visible by counterstaining with hematoxylin (×100/×400 original magnification). The *black arrows* indicate COX-2-positive cells in the liver parenchyma. The *white arrows* point to COX-2-positive cells within the tumor microenvironment (lower images, 400-fold magnification). Tumor cells are COX-2 negative. *Bar* 50 μm

COX-2 localization in liver tissue

Immunofluorescence staining

Double immunofluorescence staining was performed using the polyclonal (ab15191) and/or monoclonal (33/Cox-2) COX-2 antibody combined with antisera specific for CK-19, Hep Par-1, ED1 or ED2.

In healthy adult rat liver, the bile duct epithelial cells were strongly positive for CK-19, a typical bile duct cell antigen. CK-19$^+$ cells were COX-2$^-$ as were Hep Par1$^+$ hepatocytes (Fig. 2a, b). Only ED1$^+$/ED2$^+$ cells (tissue macrophages) in normal liver parenchyma were COX-2$^+$ (Fig. 2c).

After administration of the toxins (TAA or CCl_4), an increasing number of ED1$^+$/ED2$^-$ mononuclear cells became detectable in the areas of damage. These cells showed only a weak positivity for COX-2. In contrast, the ED1$^+$/ED2$^+$ cells of the non-damaged tissue were clearly COX-2$^+$. There was no difference in the distribution between ED1$^+$ and COX-2$^+$ cells (Fig. 3).

The cell counting performed in both models (TAA and CCl_4) of liver damage showed a significant increase of the total number of ED1$^+$/COX-2$^+$ cells after 24 h (1.4-fold) as well as after 48 h (1.86-fold).

ED1$^+$/COX-2$^+$ cells located in the non-damaged area were ED2$^+$ as well. Their number was not significantly altered after 24 h (1.08-fold) and 48 h (0.73-fold) in comparison with the control.

ED1$^+$/COX-2$^+$ cells located in the damaged area were predominantly ED2$^-$ and only a few cells with a weak ED2$^+$ were detectable. These cells showed a significant increase after 24 h (4.29-fold) and after 48 h (12-fold).

In chronically injured livers a strong increase of CK-19$^+$ cells is observable but these CK-19$^+$ cells remained COX-2$^-$ as did those localized within the CC region (Fig. 4a). However, COX-2$^+$ and ED1$^+$/ED2$^+$ cells were observed within the "regenerating" nodules. While ED1$^+$/ED2$^+$ cells within the regenerating nodules strongly correlated with COX-2$^+$ cells (ED1 and COX-2 co-localization), ED1$^+$/ED2$^-$ cells within the CC region were COX-2$^-$ (Fig. 4c).

In human cirrhotic livers, co-expression of CD68 (tissue macrophages) and COX-2 was confirmed in the "regenerating" nodules, whereas no co-expression of Hep Par-1 and COX-2, nor of CK-19 and COX-2 were observed (Fig. 5). There was no difference between cirrhotic livers after developing HCC or CC and cirrhotic livers without tumor.

Immunohistochemistry by APAAP method

After specificity analysis performed by 2-DE Western blot analysis and characterisation of the identified proteins we realized the potentially non-specific binding of other proteins.

For immunohistochemistry with the APAAP method, we used the COX-2 monoclonal antibody (33/Cox-2). The results of APAAP staining of acute damaged livers confirmed the results of immunofluorescence staining. Nonspecific staining, particularly in the area of injury ("inflamed hepatocytes"), did not appear (Fig. 6).

In the chronically damaged liver (tumor region), some weakly COX-2$^+$ cells were detectable within the tumor microenvironment (Fig. 7).

COX-2 gene expression in a macrophage cell line RAW 264.7 and in isolated rat liver cells

Specifity of the antibodies was controlled by using proteins from macrophage cell line RAW 264.7 and isolated rat liver macrophages. RAW 264.7 cells do not constitutively express COX-2. However, the protein can be quickly induced by treatment of the cells with endotoxin (Fig. 8a). COX-2 protein was tested in isolated rat liver cells using Western blotting (Fig. 8b). Specific COX-2 protein band (70 kDa) was clearly visible only in cultured Kupffer cells 24 h after plating. As also isolated resident tissue macrophages constitutively express COX-2 gene treatment with LPS aimed to show that COX-2 gene expression can be further upregulated. RT-PCR analysis of total RNA revealed an increase of COX-2 gene expression in isolated Kupffer cells after LPS-administration (Fig. 8c). COX-2 protein in isolated fraction 3 (inflammatory) and 4 (resident) macrophages showed a higher total protein amount in fraction 4 than in fraction 3 48 h after CCl_4-induced acute liver injury (Fig. 8d).

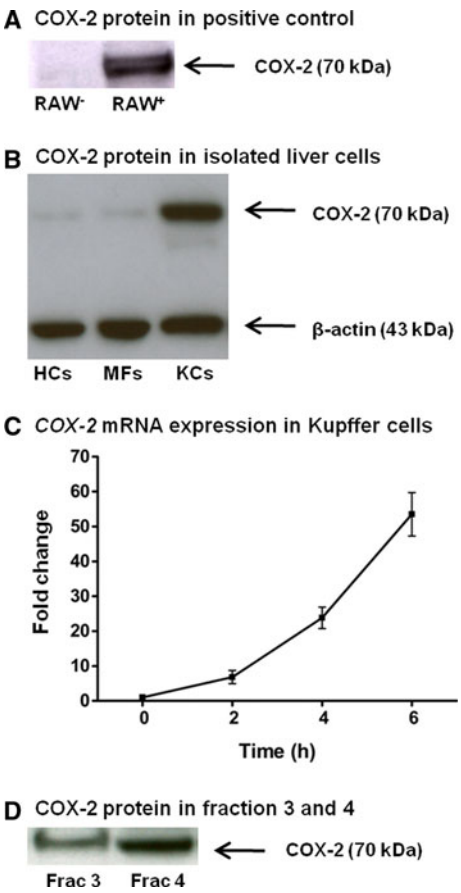

Fig. 8 **a** COX-2 antibody binding was tested using protein from macrophage cell line RAW 264.7 as a positive control. Total protein extracts from unstimulated cells (RAW$^-$) and LPS/PMA-stimulated cells (RAW$^+$) were analyzed. **b** COX-2 protein expression in hepatocytes (HCs), (myo)fibroblasts (MFs), and Kupffer cells (KCs) isolated from rat liver. COX-2 protein (70 kDa) is clearly visible in isolated KCs. β-actin (43 kDa) was used as an internal standard. **c** *COX-2* mRNA expression increases in isolated Kupffer cells after LPS-administration. **d** Shown is the COX-2 protein amount in isolated macrophages after CCl_4-induced acute liver injury of fractions 3 (inflammatory macrophages) and 4 (resident macrophages)

2-DE Western blot analysis and specificity of antibodies

The specificity of the COX-2 antibodies was verified by 2-DE Western blot analysis and subsequently by mass spectrometric identification of the corresponding spots in silver-stained gels. We used total protein lysates from rat liver and from RAW 264.7 cell line (as a positive control). We tested three different polyclonal COX-2 antibodies (ab15191, sc-1746, sc-7951) and one monoclonal COX-2 antibody (33/Cox-2).

Total protein of rat liver

The polyclonal antibody SC1746 revealed two clearly visible protein spots. One of these spots could be successfully identified by mass spectrometry as Vimentin (VIME). The polyclonal antibody SC7951 showed five protein spots. Two of these spots could be successfully identified as Procollagen-lysine, 2-oxoglutarate 5-dioxygenase 3 (PLOD3), and heat shock 70 kDa protein 1A/1B (HSP71). The third tested polyclonal antibody (ab15191) showed up several clearly visible protein spots (Fig. 9, left side). The mass spectrometric identification of 12 protein spots revealed six different proteins (DnaJ homolog subfamily C member 3 (DNJC3), Alpha-enolase (ENOA), D-3-phosphoglycerate dehydrogenase (SERA), Arginase-1 (ARGI1), Cystathionine gamma-lyase (CGL), and Fructose-bisphosphate aldolase B (ALDOB)). Arginase 1 was represented by six different protein spots. The monoclonal antibody (33/Cox-2) showed no specific signal (data not shown). Neither the polyclonal nor the monoclonal antibody detected COX-2 from the 2-DE-gel containing total protein lysates from rat liver.

Overall, a good correlation was found between the observed and the calculated isoelectric point and molecular weight of the identified proteins (Table 2; Suppl. Table 1).

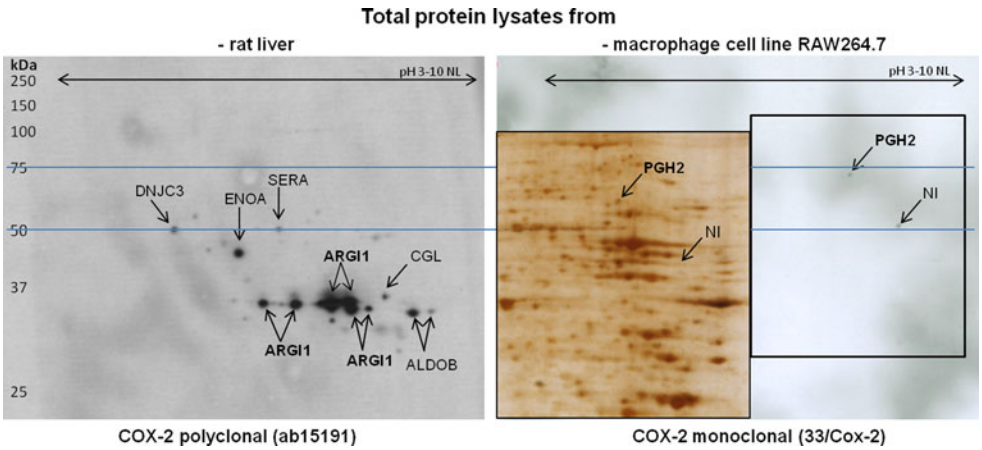

Fig. 9 Shown are the results from 2-DE Western blot analysis. After ECL staining numerous spots are visible when the polyclonal antibody (ab15191) and total protein from rat liver were used (*left side*). A spot in the field of 70 kDa is not visible. The results of mass spectrometry are indicated in the figure and marked with *arrows*. Using total protein of the macrophage cell line RAW 264.7, two spots were visible (*right side*). While one spot (in the range of 50 kDa) could not be located in the silver-stained gel (*small box*), the evaluation of the second spot (in the range just below 75 kDa) resulted in COX-2 (prostaglandin synthase 2, PGH2). *NI* not identified

Total protein from the RAW 264.7 cell line

As a positive control, the total protein lysate of the macrophage cell line RAW 264.7 was used. The review of the polyclonal (ab15191) and monoclonal (33/Cox-2) antibody revealed a specific signal in the range of 70 kDa for both antibodies. While the monoclonal antibody, however, showed two spots in the region of 70 kDa, the polyclonal antibody showed several additional spots in the range of 30–80 kDa, as was observable when total protein lysates from rat liver tissue were used. The two spots of the monoclonal antibody were examined by mass spectrometry. One protein spot could be successfully identified as Chain A, Cyclooxygenase-2 (Prostaglandin Synthase-2) complexed with a non-selective Inhibitor, Flurbiprofen (PGH2) (Fig. 9, right side; Table 3; Suppl. Table 1). For the second spot no corresponding protein spot in the silver-stained gel was found.

Discussion

In this study we show that COX-2 is constitutively expressed in macrophages of normal liver tissue and that COX-2 gene expression increases in acutely, as well as in chronically damaged liver in two rat models. Two different models of liver injury were studied in an attempt to show that COX-2 gene is expressed in mononuclear phagocytes of healthy and damaged liver independently of the toxin used as well as in human liver tissue. The increase is due to the increased expression in the resident liver tissue macrophages and to recruited inflammatory mononuclear phagocytes. Contrary to what we expected, COX-2 immuno-detection in tumoral tissue is not found in tumoral cells but only in those macrophages of the tumor microenvironment and of the non tumoral tissue. The constitutive COX-2 expression in tissue macrophages was confirmed in isolated rat Kupffer cells. The results obtained by the in vitro treatment of Kupffer cells with LPS indicates that the COX-2 expression can be further stimulated in resident macrophages as suggested by the data obtained in vivo.

COX-2 mRNA expression showed a significant increase at different time points after TAA administration with a maximum value after 24 h and during chronic liver injury starting from 8 weeks of TAA administration. According to immunohistology, this increase was not due to either the "inflamed" hepatocytes (cells located around the inflamed areas) (Chariyalertsak et al. 2001; Giannitrapani et al. 2009) or to the CC cells (Endo et al. 2002).

Administration of TAA or CCl_4, two well-known hepatotoxicants, altered not only epithelial cells, but also provoked centrilobular inflammation/necrosis. The inflamed areas were populated mainly by infiltrating monocytes/macrophages, identified by ED1 antigen expression (Neubauer et al. 2008; Laskin et al. 2011; Zborek et al. 2006). In order to demonstrate that recruited inflammatory mononuclear phagocytes may also be responsible for the increase of COX-2 gene expression, double immunofluorescence staining studies were performed using anti-ED1, anti-ED2 (Ramadori and Saile 2004), and anti-COX-2-antibodies. Interestingly, COX-2 positivity was found not only in the $ED1^+/ED2^+$ (resident) macrophages but also in the $ED1^+/ED2^-$ mononuclear phagocytes of the damaged areas and of the tumor microenvironment. The presence of the COX-2 protein was confirmed in isolated inflammatory phagocytes. In the past, COX-2 positivity in mononuclear cells located within the tumor microenvironment was not

Table 2 Isoelectric point (pI), molecular weight (MW), and function of identified proteins in liver proteome using the indicated COX-2 antibodies

Protein name	Spot label	pI obs./calc.	MW (kDa) obs./calc.	Function
COX-2 Abcam (ab15191), rabbit polyclonal				
DnaJ homolog subfamily C member 3	DNJC3_RAT	5.8/5.62	51/57.5	Involved in the unfolded protein response (UPR) during ER stress
Alpha-enolase	ENOA_RAT	6.6/6.16	47/47.1	Carbohydrate metabolism; glycolysis
D-3-phosphoglycerate dehydrogenase	SERA_RAT	7.1/6.30	52/56.5	Amino-acid biosynthesis
Arginase-1	ARGI1_RAT	6.9/6.76	36/35.0	Nitrogen metabolism; urea cycle. Tissue specificity: detected in liver (at protein level)
		7.3/6.76	36/35.0	
		7.7/6.76	36/35.0	
		8.0/6.76	36/35.0	
		8.2/6.76	36/35.0	
Cystathionine gamma-lyase	CGL_RAT	8.4/8.20	38/43.6	Catalyzes the last step in the transsulfuration pathway from methionine to cysteine. Converts two cysteine molecules to lanthionine and hydrogen sulfide
Fructose-bisphosphate aldolase B	ALDOB_RAT	8.8/8.67	36/39.6	Carbohydrate metabolism; glycolysis
COX-2 Santa Cruz (SC1746), goat polyclonal				
Vimentin	VIME_RAT	5.3/5.06	70/53.7	Class-III intermediate filament
COX-2 Santa Cruz (SC7951), rabbit polyclonal				
Procollagen-lysine, 2-oxoglutarate 5-dioxygenase 3	PLOD3_RAT	7.1/5.82	70/85.0	Forms hydroxylysine residues in collagens. Essential for the stability of the intermolecular collagen cross-links
Heat shock 70 kDa protein 1A/1B	HSP71_RAT	6.6/5.61	74/70.1	Stabilize proteins against aggregation and mediate the folding of newly translated polypeptides. They bind extended peptide segments during translation and membrane translocation, or following stress-induced damage
COX-2 BD Transduction Laboratories (33/Cox-2), mouse monoclonal				
./.	./.	./.	./.	./.

pI isoelectric point, *obs.* observed, *calc.* calculated

Table 3 Isoelectric point, molecular weight, and function of identified proteins in proteome of macrophage cell line RAW 264.7

Protein name	Spot label	pI obs./calc.	MW (kDa) obs./calc.	Function
COX-2 BD Transduction Laboratories (33/Cox-2), mouse monoclonal				
Chain A, Cyclooxygenase-2 (Prostaglandin Synthase-2) complexed with a non-selective inhibitor, Flurbiprofen	PGH2_MOUSE	7,3/6.86	73/67.2	Mediates the formation of prostaglandins from arachidonate

pI isoelectric point, *obs.* observed, *calc.* calculated

underlined, but it is possible that these cells were responsible for the presence of the COX-2 mRNA level measured in total RNA extracted from tissue samples (Bamba et al. 1999; Sheehan et al. 2005).

To be sure of the specificity of the different available antibodies, 2-DE and mass spectrometric analysis of COX-2-positive protein spots were performed. The lack of any specific signal in total protein lysates from rat liver for all tested COX-2 antibodies in the range of 70 kDa could be due to the small total amount of this protein and may be partly due to limitations in the method used. To ensure that 2-DE is suitable for the detection of this protein, we used (as a positive control) total protein lysates of the macrophage cell line RAW 264.7. And indeed, a specific binding

of the monoclonal antibody (33/Cox-2) to COX-2 protein could be detected by mass spectrometry. However, the COX-2 protein spot in the total protein lysate of the macrophage cell line was a rather small protein spot. This could be interpreted as a further indication of an only limited total amount of this protein. This assumption is supported by the absence of COX-2 detection in various other studies of proteome of the liver conducted to date (Kawase et al. 2009; Li et al. 2004; Sun et al. 2010).

The results of 2-DE were reflected also in immunohistochemistry. The monoclonal antibody (33/Cox-2), whose specific binding could be demonstrated, was strictly correlated with $ED1^+$ cells. In contrast, the polyclonal antibody (ab15191) showed not only a clear correlation with $ED1^+$ cells, but also a weak positivity in hepatocytes. However, this antibody also binds to other proteins, including ARGI1. ARGI1 is involved in the urea cycle and appears to play a role in liver injury and NO synthesis (Reid et al. 2007). In a recent study, ARGI1 was introduced as a possible new immunohistochemical marker for hepatocytes and hepatocellular neoplasms (Yan et al. 2010). This may explain the weak hepatocyte positivity detectable in the present study using the polyclonal COX-2 antibody (ab15191).

Similar results are obtained with two other tested polyclonal COX-2 antibodies (SC1746, SC7951). Infact, vimentin (VIME) was detected by the polyclonal COX-2 antibody SC1746 and recently described as a potential biomarker for HCC (Sun et al. 2010). Furthermore, COX-2 expression was described in hepatocytes during liver regeneration using COX-2 antibody SC7951 (Fernández-Martínez et al. 2004). This antibody, however, in our hands also binds to HSP71 which is upregulated in hepatocytes in liver regeneration (Brockmann et al. 2005; Shi et al. 2007). These potentially non-specific bindings, depending on the antibodies used, may explain the conflicting results reported in the literature regarding the hepatic COX-2 expression.

Conclusion

This work shows that COX-2 is constitutively expressed in tissue macrophages of rat and human liver. Increase of COX-2 gene expression in damaged liver tissue is due to increased expression in resident macrophages and inflammatory cells which are also present in tumoral tissue. Cholangiocarcinoma cells of this model are COX-2 negative. The contribution of mononuclear phagocytes should be taken into account when total RNA extracted from tumoral tissue is studied.

Acknowledgments We greatly appreciate the skillful technical assistance of Mrs. D. Fey and C. Dunaiski. We thank Dr. Lüder from the Dept. of Bacteriology, Georg-August-University Goettingen, Germany, for the RAW 264.7 cell line. We thank Professor H. Urlaub from the MPI Goettingen for mass spectrometric identification of the samples. The contribution of Dr. Marta Wójcik in this study was supported by Grant no. N N308 3169 33 from the Ministry of Science and Higher Education, Poland.

Conflict of interest The authors of this manuscript have no conflicts of interest to disclose.

References

Ahmad N, Chen LC, Gordon MA, Laskin JD, Laskin DL (2002) Regulation of cyclooxygenase-2 by nitric oxide in activated hepatic macrophages during acute endotoxemia. J Leukoc Biol 71:1005–1011

Armbrust T, Schwogler S, Zohrens G, Ramadori G (1993) C1 esterase inhibitor gene expression in rat Kupffer cells, peritoneal macrophages and blood monocytes: modulation by interferon gamma. J Exp Med 178:373–380

Bamba H, Ota S, Kato A, Adachi A, Itoyama S, Matsuzaki F (1999) High expression of cyclooxygenase-2 in macrophages of human colonic adenoma. Int J Cancer 83:470–475

Bayly CI, Black WC, Leger S, Ouimet N, Ouellet M, Percival MD (1999) Structure-based design of COX-2 selectivity into flurbiprofen. Bioorg Med Chem Lett 9:307–312

Bennett A, Del Tacca M, Stamford IF, Zebro T (1977) Prostaglandins from tumors of human large bowel. Br J Cancer 35:881–884

Betz M, Fox BS (1991) Prostaglandin E2 inhibits the production of Th1 lymphokines but not Th2 lymphokines. J Immunol 146:108–113

Blum H, Beier H, Gross HJ (1987) Improved silver staining of plant proteins, RNA and DNA in polyacrylamide gels. Electrophoresis 8:93–99

Bradford MM (1976) A rapid and sensitive method for the quantitation of microgram quantities of protein using the principle of protein-dye binding. Anal Biochem 72:248–254

Brockmann JG, August C, Wolters HH, Hömme R, Palmes D, Baba H, Spiegel HU, Dietl KH (2005) Sequence of reperfusion influences ischemia/reperfusion injury and primary graft function following porcine liver transplantation. Liver Transpl 11:1214–1222

Casado M, Molla B, Roy R, Fernández-Martínez A, Cucarella C, Mayoral R, Boscá L, Martín-Sanz P (2007) Protection against Fas-induced liver apoptosis in transgenic mice expressing cyclooxygenase 2 in hepatocytes. Hepatology 45:631–637

Chariyalertsak S, Sirikulchayanonta V, Mayer D, Kopp-Schneider A, Fürstenberger G, Marks F, Müller-Decker K (2001) Aberrant cyclooxygenase isozyme expression in human intrahepatic cholangiocarcinoma. Gut 48:80–86

Cordell JL, Falini B, Erben WN, Gosh AK, MacDonald S, Pulford KA, Stein H, Mason DY (1984) Immunoenzymatic labeling of monoclonal antibodies using immune complexes of alkanine phosphatase and monoclonal anti-alkaline phosphatase (APAAP complexes). J Histochem Cytochem 32:219–229

Eisinger AL, Prescott SM, Jones DA, Stafforini DM (2007) The role of cyclooxygenase-2 and prostaglandins in colon cancer. Prostaglandins Other Lipid Mediat 82:147–154

Endo K, Yoon BI, Pairojkul C, Demetris AJ, Sirica AE (2002) ERBB-2 overexpression and cyclooxygenase-2 up-regulation in human cholangiocarcinoma and risk conditions. Hepatology 36:439–450

Fernández-Martínez A, Callejas NA, Casado M, Boscá L, Martín-Sanz P (2004) Thioacetamide-induced liver regeneration involves the expression of cyclooxygenase 2 and nitric oxide synthase 2 in hepatocytes. J Hepatol 40:963–970

Gasparini G, Longo R, Sarmiento R, Morabito A (2003) Inhibitors of cyclo-oxygenase 2: a new class of anticancer agents? Lancet Oncol 4:605–615

Giannitrapani L, Ingrao S, Soresi M, Florena AM, La Spada E, Sandonato L, D'Alessandro N, Cervello M, Montalto G (2009) Cyclooxygenase-2 expression in chronic liver diseases and hepatocellular carcinoma: an immunohistochemical study. Ann N Y Acad Sci 1155:293–299

Han C, Wu T (2005) Cyclooxygenase-2-derived prostaglandin E2 promotes human cholangiocarcinoma cell growth and invasion through EP1 receptor-mediated activation of the epidermal growth factor receptor and Akt. J Biol Chem 280:24053–24063

Han C, Leng J, Demetris AJ, Wu T (2004) Cyclooxygenase-2 promotes human cholangiocarcinoma growth: evidence for cyclooxygenase-2-independent mechanism in celecoxib-mediated induction of p21 waf1/cip1 and p27kip1 and cell cycle arrest. Cancer Res 64:1369–1376

Hla T, Neilson K (1992) Human cyclooxygenase-2 cDNA. Proc Natl Acad Sci 89:7384–7388

Hu KQ (2003) Cyclooxygenase 2 (COX-2)-prostanoid pathway and liver diseases. Prostaglandins Leukotrienes Essent Fat Acids 69:329–337

Kawase H, Fujii K, Miyamoto M, Kubota KC, Hirano S, Kondo S, Inagaki F (2009) Differential LC-MS-based proteomics of surgical human cholangiocarcinoma tissues. J Proteome Res 8:4092–4103

Kirschenbaum A, Liotta DR, Yao S, Liu XH, Klausner AP, Unger P, Shapiro E, Leav I, Levine AC (2000) Immunohistochemical localization of cyclooxygenase-1 and cyclooxygenase-2 in the human fetal and adult male reproductive tracts. J Clin Endocr Metab 85:3436–3441

Knittel T, Armbrust T, Schwoegler S, Schuppan D, Meyer zum Buenschenfelde KH, Ramadori G (1992) Distribution and cellular origin of undulin in the rat liver. Lab Invest 67:779–787

Knittel T, Dinter C, Kobold D, Neubauer K, Mehde M, Eichhorst S, Ramadori G (1999) Expression and regulation of cell adhesion molecules by hepatic stellate cells (HSC) of rat liver: involvement of HSC in recruitment of inflammatory cells during hepatic tissue repair. Am J Pathol 154:153–167

Knook DL, Sleyster EC (1976) Separation of Kupffer and endothelial cells of the rat liver by centrifugal elutriation. Exp Cell Res 99:444–449

Kondo M, Yamamoto H, Nagano H, Okami J, Ito Y, Shimizu J, Eguchi H, Miyamoto A, Dono K, Umeshita K, Matsuura N, Wakasa K, Nakamori S, Sakon M, Monden M (1999) Increased expression of COX-2 in nontumor liver tissue is associated with shorter disease-free survival in patients with hepatocellular carcinoma. Clin Cancer Res 5:4005–4012

Kunkel SL, Chensue SW, Phan SH (1986a) Prostaglandins as endogenous mediators of interleukin 1 production. J Immunol 136:186–192

Kunkel SL, Wiggins RC, Chensue SW, Larrick J (1986b) Regulation of macrophage tumour necrosis factor production by prostaglandin E2. Biochem Biophys Res Commun 137:404–410

Kunkel SL, Spengler M, May MA, Spengler R, Larrick J, Remick D (1988) Prostaglandin E2 regulates macrophage-derived tumor necrosis factor gene expression. J Biol Chem 263:5380–5384

Laskin DL, Sunil VR, Gardner CR, Laskin JD (2011) Macrophages and tissue injury: agents of defense or destruction? Annu Rev Pharmacol Toxicol 51:267–288

Li C, Hong Y, Tan YX, Zhou H, Ai JH, Li SJ, Zhang L, Xia QC, Wu JR, Wang HY, Zeng R (2004) Accurate qualitative and quantitative proteomic analysis of clinical hepatocellular carcinoma using laser capture microdissection coupled with isotope-coded affinity tag and two-dimensional liquid chromatography mass spectrometry. Mol Cell Proteomics 3:399–409

Lüder CG, Algner M, Lang C, Bleicher N, Gross U (2003) Reduced expression of the inducible nitric oxide synthase after infection with Toxoplasma gondii facilitates parasite replication in activated murine macrophages. Int J Parasitol 33:833–844

Mansuroglu T, Baumhoer D, Dudas J, Haller F, Cameron S, Lorf T, Füzesi L, Ramadori G (2009a) Expression of stem cell factor receptor c-kit in human nontumoral and tumoral hepatic cells. Eur J Gastroenterol Hepatol 21:1206–1211

Mansuroglu T, Ramadori P, Dudás J, Malik I, Hammerich K, Füzesi L, Ramadori G (2009b) Expression of stem cell factor and its receptor c-Kit during the development of intrahepatic cholangiocarcinoma. Lab Invest 89:562–574

Mohammed NA, Abd El-Aleem SA, El-Hafiz HA, McMahon RF (2004) Distribution of constitutive (COX-1) and inducible (COX-2) cyclooxygenase in postviral human liver cirrhosis: a possible role for COX-2 in the pathogenesis of liver cirrhosis. J Clin Pathol 57:350–354

Neubauer K, Knittel T, Armbrust T, Ramadori G (1995) Accumulation and cellular localisation of fibrinogen/fibrin during short-term and longterm rat liver injury. Gastroenterology 108:1124–11135

Neubauer K, Lindhorst A, Tron K, Ramadori G, Saile B (2008) Decrease of PECAM-1-gene-expression induced by proinflammatory cytokines IFN-γ and IFN-α is reversed by TGF-β in sinusoidal endothelial cells and hepatic mononuclear phagocytes. BMC Physiol 8:9

O'Banion MK, Sadowski HB, Winn V, Young DA (1991) A serum- and glucocorticoid-regulated 4-kilobase mRNA encodes a cyclooxygenase-related protein. J Biol Chem 266:23261–23267

O'Banion MK, Winn VD, Young DA (1992) cDNA cloning and functional activity of a glucocorticoid-regulated inflammatory cyclooxygenase. Proc Natl Acad Sci 89:4888–4892

Picot D, Loll PJ, Garavito RM (1994) The X-ray crystal structure of the membrane protein prostaglanind H2 synthase-1. Nature (Lond) 367:243–249

Proctor E, Chatamra K (1982) High yield micronodular cirrhosis in the rat. Gastroenterology 83:1183–1190

Ramadori G, Saile B (2004) Inflammation, damage repair, immune cells, and liver fibrosis: specific or nonspecific, this is the question. Gastroenterology 127:997–1000

Raschke WC, Baird S, Ralph P, Nakoinz I (1978) Functional macrophages cell lines transformed by Abelson leukemia virus. Cell 15:261–267

Reid KM, Tsung A, Kaizu T, Jeyabalan G, Ikeda A, Shao L, Wu G, Murase N, Geller DA (2007) Liver I/R injury is improved by the arginase inhibitor, *N*(omega)-hydroxy-nor-L-arginine (nor-NOHA). Am J Physiol Gastrointest Liver Physiol 292:G512–G517

Schultze FC, Petrova DT, Oellerich M, Armstrong VW, Asif AR (2010) Differential proteome and phosphoproteome signatures in human T-lymphoblast cells induced by sirolimus. Cell Prolif 43:396–404

Sheehan KM, Steele C, Sheahan K, O'Grady A, Leader MB, Murray FE, Kay EW (2005) Association between cyclooxygenase-2-expressing macrophages, ulceration and microvessel density in colorectal cancer. Histopathology 46:287–295

Shevchenko A, Wilm M, Vorm O, Mann M (1996) Mass spectrometric sequencing of proteins from silver-stained polyacrylamide gels. Anal Chem 68:850–858

Shi Q, Dong Z, Wei H (2007) The involvement of heat shock proteins in murine liver regeneration. Cell Mol Immunol 4:53–57

Simmons DL, Botting RM, Hla T (2004) Cyclooxygenase isozymes: the biology of prostaglandin synthesis and inhibition. Pharmacol Rev 56:387–437

Sun S, Poon RT, Lee NP, Yeung C, Chan KL, Ng IO, Day PJ, Luk JM (2010) Proteomics of hepatocellular carcinoma: serum vimentin

as a surrogate marker for small tumors (<2 cm). J Proteome Res 9:1923–1930

Thakur P, Sanyal SN (2010) Chemopreventive action of diclofenac in dimethybenzanthracene induced lung cancer in female wistar rat. J Environ Pathol Toxicol Oncol 29:255–265

Tsujii M, Kawano S, Tsuji S, Sawaoka H, Hori M, DuBois RN (1998) Cyclooxygenase regulates angiogenesis induced by colon cancer cells. Cell 93:705–716

Williams CS, Tsujii M, Reese J, Dey SK, DuBois RN (2000) Host cyclooxygenase-2 modulates carcinoma growth. J Clin Investig 105:1589–1594

Wu T (2005) Cyclooxygenase-2 and prostaglandin signaling in cholangiocarcinoma. Biochim Biophys Acta 1755:135–150

Yan BC, Gong C, Song J, Krausz T, Tretiakova M, Hyjek E, Al-Ahmadie H, Alves V, Xiao SY, Anders RA, Hart JA (2010) Arginase-1: a new immunohistochemical marker of hepatocytes and hepatocellular neoplasms. Am J Surg Pathol 34:1147–1154

Yeh CN, Lin KJ, Hsiao IT, Yen TC, Chen TW, Jan YY, Chung YH, Lin CF, Chen MF (2008) Animal PET for thioacetamide-induced rat cholangiocarcnoma: a novel and reliable platform. Mol Imaging Biol 10:209–216

Zborek A, Malusecka E, Rusin A, Krzyzowska-Gruca S, Krawczyk Z (2006) Influx of macrophages into livers of rats treated with hepatotoxicans (thioacetamide, allyl alcohol, D-galastosamine) induced expression of HSP25. J Mol Hist 37:381–389

Zhang Z, Lai GH, Sirica AE (2004) Celecoxib-induced apoptosis in rat cholangiocarcinoma cells mediated by Akt inactivation and Bax translocation. Hepatology 39:1028–1037

Zhang X, Miao X, Tan W, Ning B, Liu Z, Hong Y, Song W, Guo Y, Zhang X, Shen Y, Qiang B, Kadlubar FF, Lin D (2005) Identification of functional genetic variants in cyclooxygenase-2 and their association with risk of esophageal cancer. Gastroenterology 129:565–576